BEAM BRIGHTNESS IMPROVEMENT BY ELLIPSOIDAL LASER SHAPING FOR CW PHOTOINJECTORS

H. Qian#, M. Krasilnikov, F. Stephan, DESY, Zeuthen, Germany

Abstract

High brightness photoinjectors operating in continuous wave (CW) mode are enabling many advanced applications, such as CW X-ray free electron laser (FEL), ERL light source, electron coolers for hadron beams and electron-ion colliders and so on. Now, three types of CW electron guns are available: DC gun, SRF gun, and normal conducting RF gun. Compared to pulsed guns, the CW gun beam brightness is compromised due to a lower acceleration gradient at the cathode. Flattop laser shaping and 'cigar beam' photoemission have been applied in CW guns to improve beam emittance. In this paper, ellipsoidal laser shaping is studied to further improve the beam brightness for CW photoinjectors towards ~0.1 μm-rad at 100 pC.

INTRODUCTION

X-ray free electron lasers (XFEL) have seen great success in the past decades, increasing peak brightness of X-ray beams over synchrotron X-ray sources by as much as 11 orders of magnitude [1]. While all current XFELs are low repetition rate pulsed machines, with advances of CW SRF linac technology, new XFEL machines in CW mode are under design [2, 3]. The gradient of a CW SRF linac is lower than a pulsed linac, and thus CW XFEL linac energy is expected to be lower. To lase at the shortest photon wavelength with lower linac energy, an even brighter electron source is required, e.g. 100 pC bunch charge with ~0.1 μm-rad transverse emittance and ~20 A peak current is wished [4].

The electron source brightness is limited by photoemission at the cathode, which can be described as [5, 6]:

$$B_{\perp}^{pancake} \propto \frac{E_0}{\sigma_{p_\perp}^2}. \quad (1)$$

$$B_{\perp}^{cigar} \propto \frac{E_0^{3/2} t_{laser}}{\sqrt{R}\sigma_{p_\perp}^2}. \quad (2)$$

where $B_{\perp}^{pancake}$ and $B_{\perp}^{cigar}$ are the transverse beam brightness for pancake photoemission and cigar photoemission, resp., E_0 is the gradient at photoemission, t_{laser} is the cathode laser pulse duration, R is the laser spot radius on the cathode, and $\sigma_{p_\perp}$ is the RMS transverse momentum after photoemission. Current CW guns, such as DC guns, SRF guns, and normal conducing guns, have a relatively low accelerating gradient at the cathode compared to pulsed guns. This makes it more difficult to achieve a better beam brightness at CW guns. According to Eq. (1) and (2), to improve the electron source brightness with a relatively low gun gradient, low $\sigma_{p_\perp}$, i.e. a low thermal emittance cathode becomes extremely important. Besides, for cigar beam photoemission, a long laser pulse duration and a smaller laser spot size can increase the transverse beam brightness by relaxing the peak current. This might be recovered by velocity or magnetic compression downstream the gun. Both methods have been applied in state of the art CW photoinjector designs.

Even with an optimized emittance at the gun, emittance growth along the linac has to be kept at a minimum. Without careful control of space charge effects, both the projected emittance growth due to slice mismatch and the slice emittance growth easily go beyond 0.1 μm-rad. Flattop laser shaping has been used to improve space charge linearization in both pulsed and CW guns. An emittance of ~0.2 μm-rad has been achieved at ~200 pC [7, 8]. To further increase the beam brightness, laser shaping for a uniform ellipsoidal beam has been proposed for 3D space charge linearization. Experimental realizations of an ellipsoidal beam have made a lot of progress in the past, both in the pancake beam regime through blowout emission and in the cigar beam regime through direct laser shaping [9-11].

In simulations, uniform ellipsoidal laser shaping has shown an emittance reduction of ~30% for a 1 nC beam compared to flattop laser shaping in high gradient pulsed guns [12]. In this paper, uniform ellipsoidal laser shaping will be applied in CW photoinjectors to check its benefit in improving the transverse emittance of a 0.1 nC beam for XFEL applications.

OPTIMIZATION TOOL

As shown in Eq. (2), the transverse beam brightness can be increased by relaxing the peak current. Besides, in CW photoinjector designs based on a DC gun or a normal conducting VHF gun, a buncher is used to control the beam peak current, trading transverse emittance.

Transverse emittance and bunch length are two compromising goals in photoinjector optimization, and a group of non-dominating optimal solutions of transverse emittance and bunch length form the Pareto front, which can be solved by multi objective genetic algorithm (MOGA) [13]. In this paper, a MOGA tool developed at LBNL is used to drive ASTRA simulations for photoinjector optimization [14]. 10000 macro particles are used in MOGA simulations, and interesting solutions are refined with 100000 macro particles in ASTRA for detailed analysis.

houjun.qian@desy.de

ISBN 978-3-95450-179-3

NC VHF GUN BASED CW PHOTOINJECTOR

A CW normal conducting VHF gun has been developed at LBNL, demonstrating a cathode gradient of 20 MV/m and a gun voltage of 750 kV. Based on the LBNL VHF gun, a CW photoinjector has been designed for the LCLS-II project. Its layout is shown in Fig. 1 [14, 15].

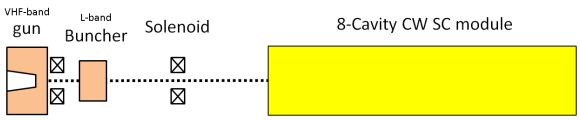

Figure 1: Normal conducting VHF gun based CW photoinjector for LCLS-II.

The LCLS-II injector has been optimized with a flattop laser and a conservative thermal emittance of 1 μm/mm. Both injector transverse emittance and peak current, satisfy LCLS-II injector specs. In this part, uniform ellipsoidal laser shaping is applied to such an injector design to further improve the beam brightness for the 100 pC case. A group of injector parameters, similar to Table 1 in Ref [15], were varied during MOGA optimizations, and optimal solutions of the Pareto fronts are shown in Fig. 2.

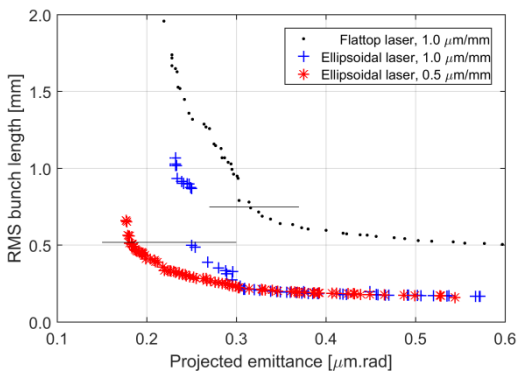

Figure 2: Pareto fronts for LCLS-II injector based on different cathode laser shaping and cathode thermal emittance with 100 pC bunch charge (10k macro particle ASTRA simulations), 20 A peak current solutions marked.

The solutions in Fig. 2 with 20 A peak current are further refined with 100k macro particle simulations. Beam projected and sliced parameters are shown in Fig. 3 and Table 1. Ellipsoidal laser shaping reduces both projected emittance and slice emittance by ~30%. With a smaller thermal emittance of 0.5 μm/mm, another 30% reduction on emittance is achieved, making ~0.1 μm-rad emittance with 20 A peak current within reach at 100 pC bunch charge. Besides emittance reduction, current profiles in Fig. 3 show, longitudinal profile distortion due to nonlinear space charge energy chirp and velocity bunching dynamics are reduced with an ellipsoidal beam. Also, the RMS bunch length for 20 A peak current is reduced from 2.5 ps to 1.7 ps.

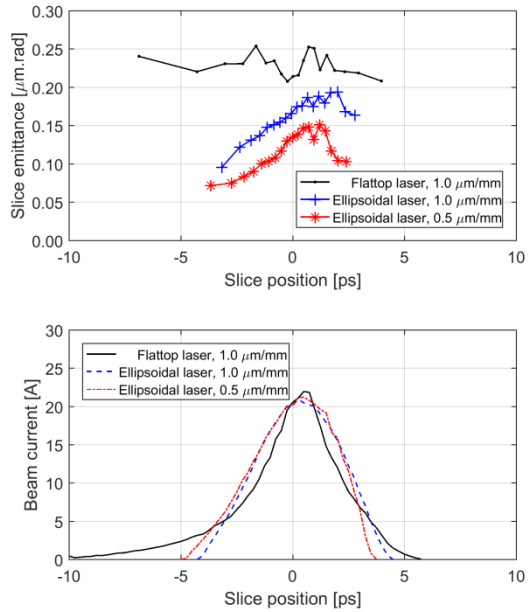

Figure 3: Slice emittance and current profile of the 20 A peak current solutions in Fig. 2 (100k macro particle simulations, each slice has 5k macro particles).

Table 1: Emittance decomposition for solutions shown in Fig. 3 ($\varepsilon_{100\%}$ is 100 % projected emittance, $\varepsilon_{95\%}$ is 95% projected emittance, $\langle\varepsilon_{slice}\rangle$ is average slice emittance, ε_{th} is thermal emittance, $\Delta\varepsilon_{mis}$ is projected emittance growth due to longitudinal slice mismatch, $\Delta\varepsilon_{slice}$ is slice emittance growth w.r.t. thermal emittance)

	Flattop 1 μm/mm	Ellipsoidal 1 μm/mm	Ellipsoidal 0.5 μm/mm	Unit
$\varepsilon_{100\%}$	0.28	0.19	0.12	μm
$\varepsilon_{95\%}$	0.22	0.14	0.09	μm
$\langle\varepsilon_{slice}\rangle$	0.23	0.16	0.11	μm
ε_{th}	0.18	0.14	0.09	μm
$\Delta\varepsilon_{slice}$	0.15	0.09	0.07	μm
$\Delta\varepsilon_{mis}$	0.16	0.09	0.04	μm

Emittance decompositions of the optimal solutions according to Ref. [16] are listed in Table 1, showing the main emittance contributions and residual emittance growth. The projected emittance is decomposed as,

$$\varepsilon_{100\%} = \sqrt{\varepsilon_{th}^2 + \Delta\varepsilon_{slice}^2 + \Delta\varepsilon_{mis}^2}\ . \qquad (3)$$

Emittance growth due to slice phase space centroid misalignment is zero in this case, because situations such as slice dependent kicks are not considered in these simulations. Table 1 shows that all solutions are dominated by thermal emittance, and that emittance growth due to slice mismatch and slice emittance growth can be reduced below 0.1 μm-rad with ellipsoidal laser.

ISBN 978-3-95450-179-3

SRF GUN BASED CW PHOTOINJECTOR

Superconducting (SC) RF is a natural CW technology. SRF guns for CW XFEL and ERL applications have been under development and great progress has been made towards high gradient operation and towards compatibility with high QE cathodes [17]. Figure 4 shows a classical photoinjector layout consisting of a 1.5 cell L-band SRF gun and an 8-cavity CW superconducting module. A superconducting solenoid is positioned at 0.5 meter from the cathode. Such an injector is used to check the effect of ellipsoidal laser shaping on the transverse emittance at 100 pC.

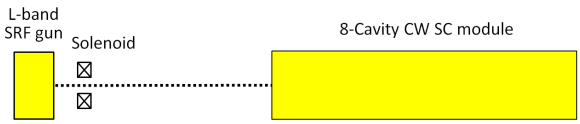

Figure 4: L-band superconducting RF gun based CW photoinjector layout (preliminary example, not optimal).

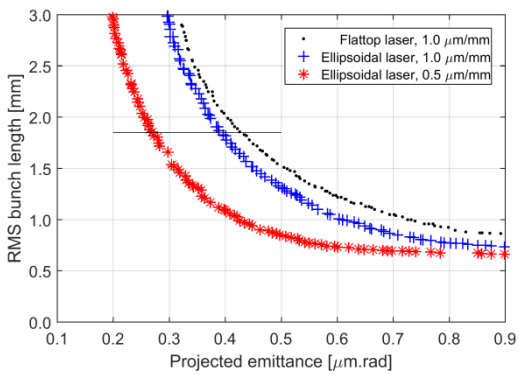

Figure 5: Pareto fronts for the CW injector in Fig. 4 with 100 pC bunch charge, 5 A peak current solutions marked.

Velocity bunching is not used in such an injector not only for simplicity but also for minimizing the longitudinal beam distortion which occur with velocity bunching. Beam bunch length is controlled by either cathode laser pulse duration or magnetic bunch compression after the harmonic cavity (see European XFEL injector [18]). During MOGA optimizations, cathode laser pulse duration and radius, solenoid strength, and SC cavity gradients can be varied for optimal solutions. The gun is set to 40 MV/m peak cathode gradient and maximum energy gain phase. Such a high field in SRF guns is still to be demonstrated in reality. On axis peak acceleration gradients of SC cavities are up to 32 MV/m, following the LCLS-II parameters [19], and the cavity phases are set to on-crest. Pareto fronts of the above injector are shown in Fig. 5, and refined 100k particle simulations are in Fig. 6 and Table 2.

Emittance decompositions of the 5 A peak current solutions show that emittance growth due to slice mismatch is negligible, which means a very good emittance compensation. Emittance growth for all three cases is dominated by slice emittance growth, caused by solenoid spherical aberration [20]. In the current setup, both the Pareto fronts and specific solutions show the ellipsoidal laser shaping effect on emittance improvement is small. With an improved solenoid design and injector layout optimization, the effect of ellipsoidal laser shaping will be further investigated.

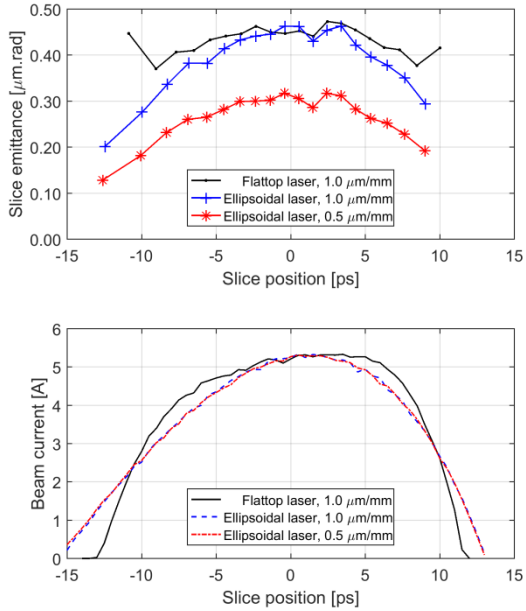

Figure 6: Slice emittance and current profile of the 5 A peak current solutions in Fig. 5.

Table 2: Emittance decomposition for solutions in Fig. 6

	Flattop 1 μm/mm	Ellipsoidal 1 μm/mm	Ellipsoidal 0.5 μm/mm	Unit
$\varepsilon_{100\%}$	0.44	0.39	0.26	μm
$\varepsilon_{95\%}$	0.35	0.31	0.21	μm
$\langle\varepsilon_{slice}\rangle$	0.43	0.38	0.26	μm
ε_{th}	0.28	0.28	0.18	μm
$\Delta\varepsilon_{slice}$	0.33	0.26	0.19	μm
$\Delta\varepsilon_{mis}$	0.08	0.05	0.03	μm

CONCLUSION

In this paper, beams from uniform ellipsoidal shaped lasers are simulated for CW photoinjectors based on a VHF gun and an L-band SRF gun for the 100 pC case. In the case of LBL type VHF gun with a peak gradient of 20 MV/m at cathode, ellipsoidal laser shaping can improve both emittance and longitudinal current profile distortions at 20 A peak current based on the LCLS-II injector. For the L-band 1.5 cell SRF gun with a 40 MV/m cathode gradient and a SC solenoid 0.5 meter from cathode, simulations show slice emittance growth is dominated by solenoid spherical aberrations. Further improvements of CW solenoid design or injector layout are needed for showing the effect of ellipsoidal laser shaping.

REFERENCES

[1] W.A. Barletta *et al.*, Nucl. Instr. Meth., 618, 69, 2010.

ISBN 978-3-95450-179-3

[2] J.N. Corlett *et al*., in *Proc. IPAC'11*, pp. 775.
[3] T.O. Raubenheimer., in *Proc. IPAC'15*, pp. 2434.
[4] Report of the Basic Energy Sciences Workshop on the Future of Electron Sources, 2016, https://science.energy.gov/~/media/bes/pdf/reports/2017/Future_Electron_Source_Worskhop_Report.pdf
[5] Ivan V. Bazarov *et al*., PRST AB 102, 104801, 2009.
[6] D. Filippetto *et al*., PRST AB 17, 024201, 2014.
[7] M. Krasilnikov *et al*., PRST AB 15, 100701, 2012.
[8] T. Schietinger *et al*., PRST AB 19, 100702, 2016.
[9] P. Musumeci *et al*., PRL 100, 244801, 2008.
[10] Yuelin Li *et al*., PRST AB 12, 020702, 2009.
[11] J. Good *et al*., "Preliminary On-Table and Photoelectron Results from the PITZ Quasi-Ellipsoidal Photocathode Laser System", presented at FEL'17, Santa Fe, NM, Aug. 2017, paper WEP006, this conference.
[12] M. Khojoyan *et al*., in *Proc. FEL'13*, pp. 298.
[13] Ivan V. Bazarov *et al*., PRST AB 8, 034202, 2005.
[14] C. F. Papadopoulos *et al*., in *Proc. FEL'14*, pp. 864.
[15] C. Mitchell *et al*., in *Proc. IPAC'16*, pp. 1699.
[16] C. Mitchell, arXiv:1509.04765.
[17] J. Sekutowicz, in *Proc. SRF'15*, pp. 994.
[18] F. Brinker, in *Proc. IPAC'16*, pp. 1044.
[19] D. Gonnella *et al*., in *Proc. IPAC'17*, pp. 1156.
[20] Ivan V. Bazarov *et al*., PRST AB 8, 034802, 2005.

ISBN 978-3-95450-179-3